51st AIAA Aerospace Sciences Meeting including the New Horizons Forum and Aerospace Exposition
07 - 10 January 2013, Grapevine (Dallas/Ft. Worth Region), Texas

AIAA 2013-1210

Actuator Line Aerodynamics Model with Spectral Elements

Yulia Peet*, Paul Fischer†, Guenter Conzelmann‡, and Veerabhadra Kotamarthi§

Arizona State University, 501 E. Tyler Mall, Tempe, AZ 85287

Argonne National Laboratory, 9700 South Cass Avenue, Argonne, IL 60439

Actuator line aerodynamics (AL) model is becoming increasingly popular for characterization of the flow field and the turbulent wakes created by the rotated turbines. AL model does not require boundary layer resolution and is thus significantly more efficient than the fully-resolved computations. Potential of this model to be applied to the simulation of really large wind plants creates the need of exploring its applicability and performance with highly-scalable computation codes. In this paper, we present the details of implementation and validation of the actuator line aerodynamics model in a high-order spectral-element code which is known to scale efficiently to hundreds of thousands of processors.

I. Introduction

Wind turbines are known to interact with the incoming free-stream in a complex manner, creating strong wakes that interfere with the performance of the turbines situated in a second raw and beyond. Accurate characterization of the wakes is important in order to predict and optimize the performance of wind turbines arranged in a larger wind farm. Large Eddy Simulations of wind turbine arrays is a promising technique with the potential of yielding a reliable data concerning the flow patterns as well as the energy output of turbines in a wind plant, and several attempts at characterizing performance of wind turbine arrays with LES have been undertaken.[1,2,3,4,5]

Due to the fact that fully-resolved simulations would be prohibitively expensive for wind turbine arrays, researchers have been employing reduced-order aerodynamics models to represent the effect of the rotating blades on the flow. The early theories describing the behavior of propellers are known as momentum theory and go back to the late 19th century with the works of Rankine,[6] Froude, Drzewiecki and others.[7] It was later extended by Glauert[8] into a blade-element momentum theory (BEM) to account for non-uniformities along the blade, such as shape, chord, twist etc. BEM method was adopted to use with wind turbine simulations as an actuator disk method,[9] and extended to a generalized actuator disk method.[10,11] Generalized actuator disk method was used in some of the earlier-cited LES studies of wind turbine arrays.[1,2]

An improvement to a generalized actuator disk method was introduced by Sørensen & Shen[12] and further developed by Troldborg[13] in the form of an actuator line aerodynamics (AL) method. The major change with respect to an actuator disk model is abandoning the circumferential symmetry of the induced force field and arriving at a fully three-dimensional model which accounts for the rotating blades as separate rotating lines. AL method is currently the most advanced model for the rotating blade aerodynamics and was used in the recent Large Eddy Simulations of Lillgrund wind plant containing 48 turbines by Churchfield et al.[4,5]

The promises of the actuator line aerodynamics model to accurately simulate the dynamics of the flow field in really large wind farms creates the motivation for introducing this model into the fluid dynamics

*Assistant Professor, School for Engineering of Matter, Transport and Energy (SEMTE), Arizona State University; also Assistant Computational Scientist, Mathematics and Computer Science Division (MCS), Argonne National Laboratory; E-mail: ypeet@asu.edu

†Senior Computational Scientist, Mathematics and Computer Science Division (MCS), Argonne National Laboratory

‡Director, Center for Energy, Environmental, and Economic Systems Analysis (CEEESA), Decision and Information Sciences Division (DIS), Argonne National Laboratory

§Atmospheric Scientist, Environmental Science Division (EVS), Argonne National Laboratory

codes which are known to be scalable for hundreds of thousands of processors. Spectral-element code Nek5000 developed at Argonne National Laboratory is one of such codes that sustained 70% parallel efficiency during LES simulations of a 217-pin subassembly on 131,072 processors on ANL IBM supercomputer Blue Gene/P,[14,15] and 71% efficiency on 262,000 processors on Jülich IBM Blue Gene/P machine during the Extreme Scaling Workshop at the Jülich Supercomputing Center in Germany[16,17] .

In this paper, we demonstrate the application of the Actuator Line Aerodynamics model to a spectral-element code Nek5000. We describe the main details of the model and its implementation, as well as present comparison with the data published in the Ph.D. thesis of Trodlborg.[13] Conclusions and future work are also discussed.

II. Numerical Method

Spectral element method (SEM) is a high-order weighted residual technique that combines the geometric flexibility of finite elements with the rapid convergence and tensor-product efficiencies of global spectral methods. In a spectral element formulation, the computational domain Ω is subdivided into nonoverlapping subdomains, or elements, $\Omega = \cup_{k=1}^{K} \Omega_k$. Each Ω_k is the image of the reference subdomain under a mapping $\boldsymbol{x}^k(\boldsymbol{r}) \in \Omega_k \rightarrow \boldsymbol{r} \in \hat{\Omega}$, with a well-defined inverse $\boldsymbol{r}^k(\boldsymbol{x}) \in \hat{\Omega} \rightarrow \boldsymbol{x} \in \Omega_k$, where the reference subdomain $\hat{\Omega} = [-1,+1]^d$. Scalar functions within each element Ω_k are represented in terms of tensor-product polynomials on Gauss-Lobbato-Legendre points on a reference subdomain $\hat{\Omega}$, which, for example, in two dimensions looks like

$$f(\boldsymbol{x})|_{\Omega_k} = \sum_{i=0}^{N} \sum_{j=0}^{N} f_{ij}^k \, h_i(r_1) \, h_j(r_2), \;\; r_1, r_2 \in [-1,+1]^2, \tag{1}$$

where $h_i(r)$ is the Lagrange polynomial of degree N satisfying $h_i(\xi_j) = \delta_{ij}$, δ_{ij} is the Kronecker delta function, and $\xi_j \in [-1,+1]$, $j = 0, \ldots, N$ are the Gauss-Lobbato Legendre (GLL) quadrature points. Further details of spectral-element method can be found, for example, in Refs. 18, 19, 20, 21. Incompressible Navier-Stokes equations are solved with the backward-difference time discretization for convective terms and implicit Crank-Nicolson time discretization for viscous terms. Spatial filter removing energy from the highest modes developed in Ref. 22 serves as a hyperviscosity SGS model for the LES. Current algorithm was scrutinously optimized to achieve perfect scalability in parallel implementation with more than 200,000 processors.[14–17]

III. Actuator Line Model

Actuator line model first developed by Sørensen & Shen[12] and Troldborg[13] and later used by Churchfield et al.[4,5] was developed in the current spectral element code. The idea of the actuator line model is that the influence of the rotating blades is accounted by the body forces introduced into the flow field. Thus, resolving blades boundary layer is not required, and simple rectilinear grid can be used. In an actuator line model, the blades are divided into the elements, and the local lift and drag force experienced by each element is calculated as

$$L = \frac{1}{2} C_l(\alpha) \, \rho \, V_{rel}^2 \, c \, w, \tag{2}$$

$$D = \frac{1}{2} C_d(\alpha) \, \rho \, V_{rel}^2 \, c \, w, \tag{3}$$

where $C_l(\alpha)$, $C_d(\alpha)$ are lift and drag coefficients, α is the local angle of attack, ρ is the density, V_{rel} is the local velocity magnitude relative to the rotating blade, c is the local chord length, and w is the actuator element width. To calculate the local relative velocity magnitude V_{rel}, one needs to consider a velocity triangle for the rotating blade, see Fig. 1 and also Refs. 12, 13

$$V_{rel} = \sqrt{V_z^2 + (\Omega \, r - V_\theta)^2}, \tag{4}$$

and Ω is the rotor rotational speed, V_z and V_θ are the velocity components in the axial direction (perpendicular to the plane of rotation), and in circumferential direction (in the plane of rotation) respectively, and r is the radial coordinate of the actuator element. Local angle of attack α is computed as $\alpha = \phi - \gamma$, where ϕ is the the angle between the relative velocity V_{rel} and the rotor plane,

$$\phi = \tan^{-1} \left(\frac{V_z}{\Omega \, r - V_\theta} \right) \tag{5}$$

and γ is the local pitch angle. After the local angle of attach is determined, the element lift and drag coefficients $C_l(\alpha)$, $C_d(\alpha)$ can be determined from the lookup tables.

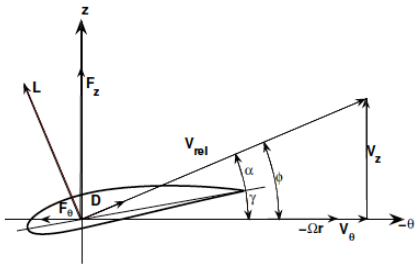

Figure 1. Velocity triangle for the determination of the local relative velocity on a turbine blade.

The next step after the local aerodynamic force $\vec{f} = L\vec{e_L} + D\vec{e_D}$ is determined, is to apply its influence, $-\vec{f}$, on the flow (here $\vec{e_L}$ and $\vec{e_D}$ are the unit vectors in the direction of the local lift and drag, respectively). To avoid singularities, the forces are distributed smoothly on several mesh points by using the Gaussian weight function

$$\eta_\epsilon(d) = \frac{1}{\epsilon^3 \pi^{3/2}} \exp\left[-\left(\frac{d}{\epsilon}\right)^2 \right] \tag{6}$$

as

$$\vec{F}(x,\, y,\, z,\, t) = -\sum_{i=1}^{N} \vec{f}(x_i,\, y_i,\, z_i,\, t)\, \eta_\epsilon(|\vec{r} - \vec{r_i}|), \tag{7}$$

where the summation is over all blade elements, x_i, y_i, z_i are the local coordinates of each blade element, and $|\vec{r} - \vec{r_i}|$ is the distance between the current point in the flow and the center of the blade element. Several studies have been considering the choice of an optimal Gaussian width ϵ.[13,23] The value of $\epsilon = 2\,w$ proposed by Troldborg[13] is used in the current study.

IV. Computational Setup

To validate the current implementation of the actuator line aerodynamics model we have closely followed the computation setup of Troldborg.[13] Our computational domain consists of a rectangular box with dimensions $(5\,R,\, 5\,R\, 10\,R)$, where R is the turbine rotor radius. Regular uniformly-spaced grid with $15 \times 15 \times 30 = 6750$ elements is used. In the current calculations the polynomial degree $N = 7$ is utilized (with 8 GLL points per element side), leading to 3.5 million grid points total. We are simulating a single three-bladed turbine closely resembling the Tjæreborg turbine studied in Ref. 13, with 30 panels across the blade radius. Steady uniform inflow is used as the inlet boundary conditions, periodic boundary conditions are employed at the spanwise direction, and free-slip at the top and bottom of the domain. Outflow boundary is treated with simple outflow conditions of zero streamwise gradients and constant pressure. The sketch of the computational domain is included in Fig. 2. Since the turbine blades are rotated within the stationary grid, the spectral interpolation routines are used to calculate the velocity values at each time step at the blade panel centers. The current calculations were run with the Reynolds number based on inflow velocity and turbine rotor radius of $Re = U_\infty R/\nu = 20,000$.

V. Results

V.A. Variation of Parameters

Before performing the validation study, it is interesting to explore the response of the flow to the variation in the model parameters, such as the tip speed ratio $\lambda = \omega R/U_\infty$, pitch angle γ, chord length c, airfoil type. For this study, we use the baseline values of parameters $\lambda = 5.05$, $\gamma = 10°$, $c = 0.065\,R$, and NACA 0018 airfoil that are constant along the blade span (which are similar but not quite the same as that of the

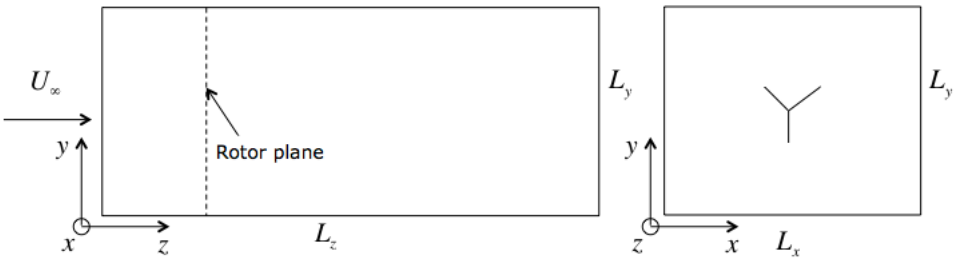

Figure 2. Sketch of the computational domain: left, front view; right, side view.

Tjæreborg turbine in Ref. 13). To investigate the influence of parameters, we vary them one at a time and observe the response of the flow.

In Fig. 3 we show the iso-surfaces of vorticity for two different tip speed ratios, $\lambda = 0.5$ and $\lambda = 5.05$. It is seen that the lower rotational rate results in a quick break-up of blade vorticity sheets, while the higher rotational rate leads to stable distinct helical tip vortices. It was shown[13] that if the rotational rate is increased even further, the tip vortices in turn break down into a small-scale turbulence, thus suggesting that the regime with the tip speed ratio of about five to seven is nearly optimum for energy extraction consistent with the Betz's law[24] and theoretical optimal rotor speed estimations.[25,26]

Similar to the tip speed ratio, the pitch angle γ also has a dramatic effect on the flow. Thus, calculations with two constant pitch angles, $\gamma = 10°$ and $\gamma = 80°$, with tip-speed ratio of $\lambda = 5.05$, are shown in Fig. 4. It is seen that turning rotor blades into the wind leads to a strongly-turbulent wake with power added to the flow rather than being extracted which can be seen from the local flow acceleration at the rotor tip in Fig. 5 a.

The influence of the chord length c and the airfoil type are more subtle, but nonetheless pronounced if one looks at the further details of the wake. Thus, varying the chord length from $0.065\,R$ to $0.2\,R$ and the airfoil type from symmetric NACA 0018 to asymmetric NACA 4418 while leaving the tip speed ratio $\lambda = 5.05$ and the pitch angle $\gamma = 10°$ did not change the vorticity pattern but led to different flow velocities in the wake. It is seen from Fig. 5 b that larger chord length leads to a larger deficit in the wake, consistent with the fact that wider blades would extract more energy from the flow. The influence of the airfoil type is the least pronounced (see Fig. 5 c, also note the change in the color levels), but it is seen that the asymmetric airfoil also tends to create a stronger wake meaning that it is more efficient at energy extraction.

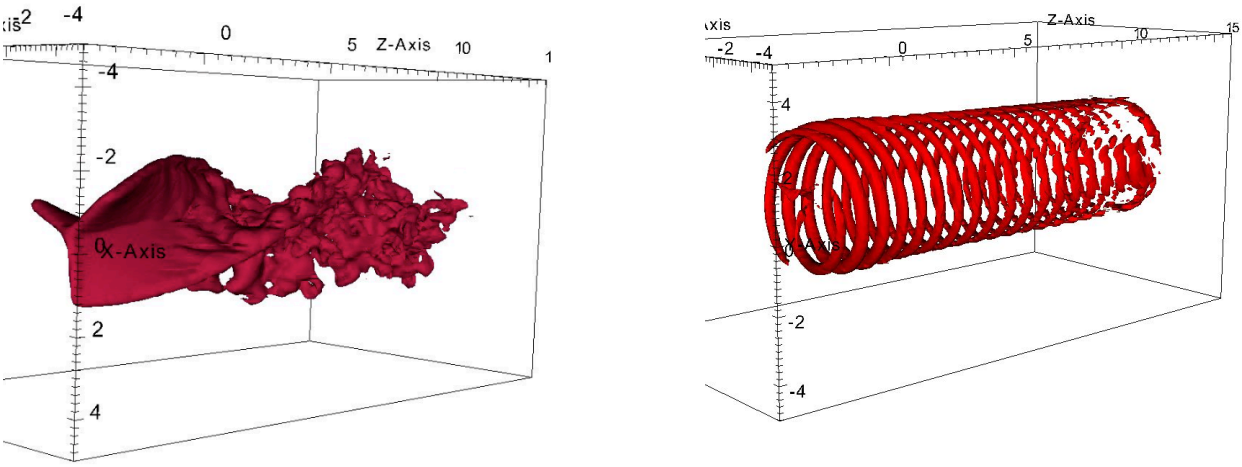

(a) $\lambda = 0.5$ (b) $\lambda = 5.05$

Figure 3. Influence of the tip-speed ratio. Iso-surfaces of vorticity are shown.

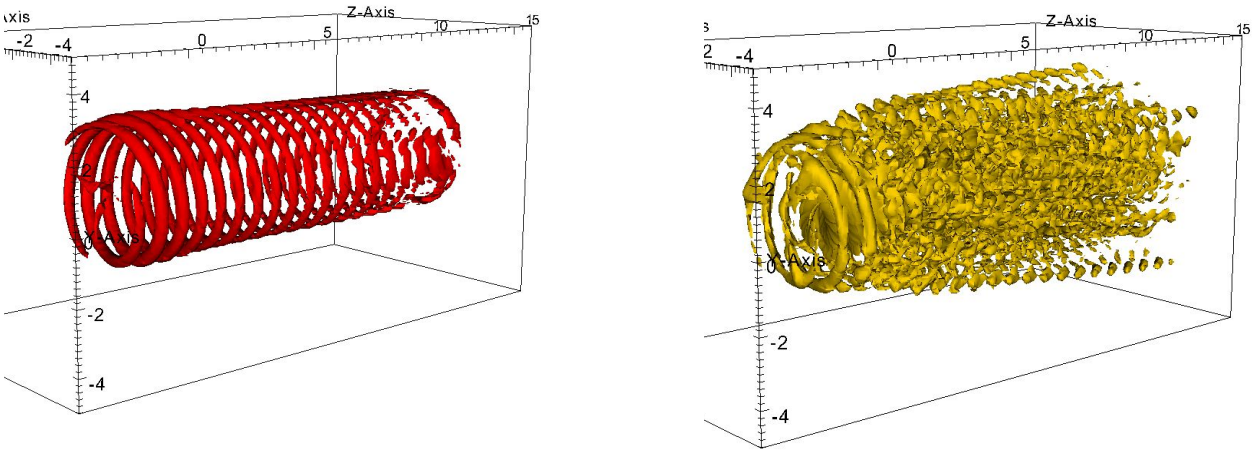

(a) $\gamma = 10°$ (b) $\gamma = 80°$

Figure 4. Influence of the pitch angle. Iso-surfaces of vorticity are shown.

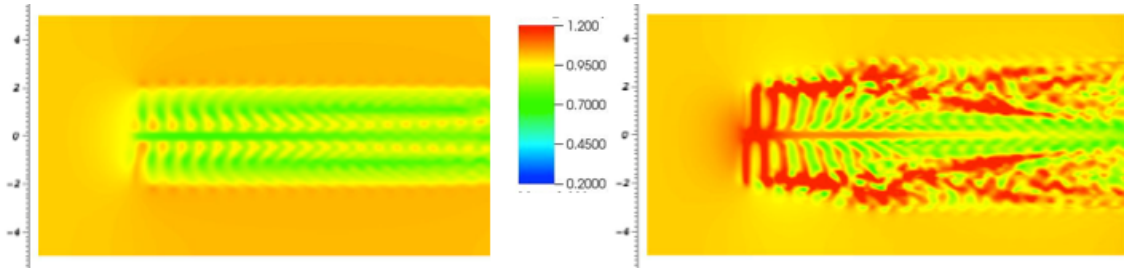

(a) Influence of the pitch angle. Left: $\gamma = 10°$; Right: $\gamma = 80°$.

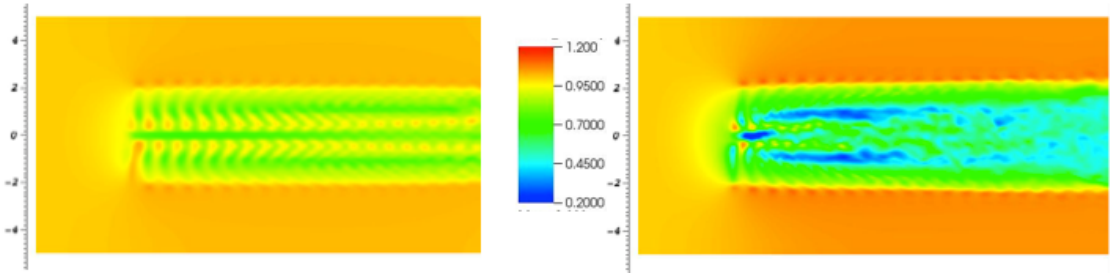

(b) Influence of the chord length. Left: $c = 0.065\,R$; Right: $c = 0.2\,R$.

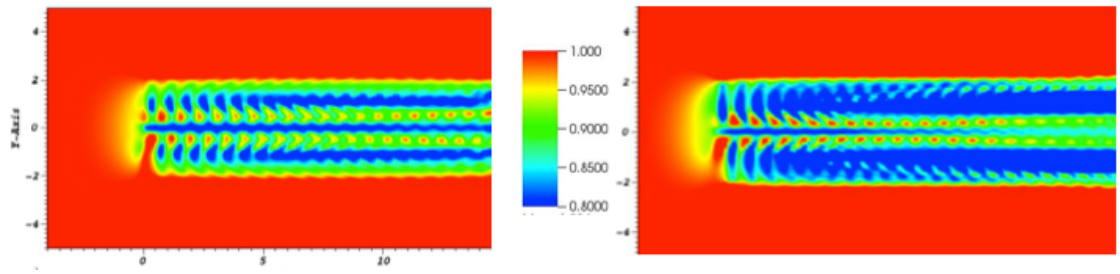

(c) Influence of the airfoil type. Left: NACA 0018; Right: NACA 4418. Note the color panel change.

Figure 5. Influence of parameters. Snapshots of instantaneous streamwise velocity at the $y - z$ centerplane are shown.

V.B. Validation

To validate the current simulations, we compare them with the simulations of Troldborg[13] performed at a very similar flow conditions. The major differences would be the Reynolds number (10^5 in Ref. 13 and $2{\cdot}10^4$ in our study) and the fact that Troldborg used varying chord length, pitch and the airfoil type ($c = 0.03 - 0.11\,R$, $\gamma = 0° - 10°$, airfoils NACA 4412–NACA 4424) while we used the constant values ($c = 0.065\,R$, $\gamma = 10°$, and either NACA 0018 or NACA 4418 airfoil). Comparison of the iso-surfaces of vorticity is presented in Fig. 6 and manifests a good agreement. Time-averaged spanwise-averaged streamwise velocity profiles across the vertical line at a distance $z = 3\,R$ downstream of the rotor are compared in Figure 7. A definite improvement in agreement is seen when symmetric NACA 0018 airfoil is replaced by the asymmetric NACA 4418 airfoil of the family used in Troldborg study. The fact that constant parameters across the blade span are considered here, and linearly varying in a Troldborg study accounts for some slight disagreements.

(a) Current calculations

(b) Calculations of Troldborg (adapted from Ref.[13])

Figure 6. Comparison of the iso-surfaces of vorticity with the data of Trodlborg.[13]

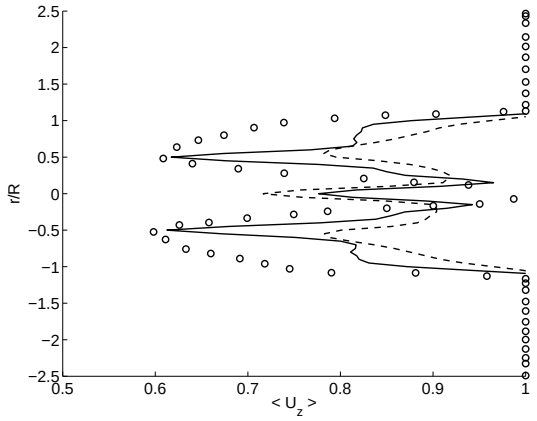

Figure 7. Comparison of time-averaged spanwise-averaged streamwise velocity profiles across a vertical line at $z/R = 3$. Solid line, NACA 4418; dashed line, NACA 0018; symbols, Troldborg.[13]

VI. Conclusions and Future Work

In this paper, we have implemented an actuator line aerodynamics model into a spectral-element code Nek5000. The response of the flow to the variation of parameters is in agreement with wind turbine aerodynamics theory and shows the tenability of the model implementation. Comparison of the time-averaged streamwise velocity profiles with the corresponding results of Troldborg[13] shows that the flow obtained with the asymmetric airfoil model is in better agreement than the one with the symmetric airfoil, consistent with the fact that asymmetric airfoils were used for the Tjæreborg wind turbine studied in Ref. 13.

The validation results presented here can be viewed as a preliminary assessment of the performance of AL model in a spectral-element simulation of wind turbine wakes. A study with the linearly-varying rotor

parameters nearly identical to those of a real Tjæreborg turbine is currently underway. Another important question is the influence of filtering and whether traditional Smagorinsky-type SGS models perform better in this type of simulations.

The current study is performed with the uniform inflow so that any uncertainty apart from the AL model itself is eliminated for a clear model validation. Considering realistic atmospheric turbulent inflow profiles and allowing for Boussinesq and boundary-layer effects in wind farm simulations would be the next step.

VII. Acknowledgements

This work was supported by the U.S. Department of Energy, Office of Energy Efficiency and Renewable Energy, through its Wind and Water Power Program at ANL. Y. P. would also like to acknowledge the support of NSF RTG grant DMS-0636574 at Northwestern University.

References

[1]Ivanell, S. S. A., *Numerical Computations of Wind Turbine Wakes*, Ph.D. thesis, Dept. of Mechanics, Gotland Univ., Stockholm, Sweden, 2010.

[2]Calaf, M., Meneveau, C., and Meyers, J., "Large Eddy Simulation Study of Fully Developed Wind-Turbine Array Boundary Layers," *Phys. Fluids*, Vol. 22, 2010, pp. 015110.

[3]Porté-Agel, F., Wu, Y.-T., and Conzemius, R. J., "Large-Eddy Simulation of Atmospheric Boundary Layer Flow Through Wind Turbines and Wind Farms," *J. of Wind Eng. and Ind. Aerodynamics*, Vol. 99, 2011, pp. 154–168.

[4]Churchfield, M. J., Lee, S., Moriarty, P. J., Martinez, L. A., Leonardi, S., Vijayakumar, G., and Brasseur, J. G., "A Large-Eddy Simulation of Wind-Plant Aerodynamics," AIAA Paper 2012-0537, 2012.

[5]Churchfield, M. J., Michalakes, J., and Moriarty, P. J., "A Numerical Study of the Effects of Atmospheric and Wake Turbulence on Wind Turbine Dynamics,," *J. Turb.*, Vol. 13, No. 14, 2012, pp. 1–32.

[6]Rankine, W. J. M., "On the Mechanical Principles of the Action of Propellers." *Trans. Inst. Naval Architects*, Vol. 6, 1865.

[7]Hansen, M. O. L., *Aerodynamics of Wind Turbines: Rotors, Loads and Structure*, London: James & James (Science Publishers) Ltd, 2001.

[8]Glauert, H., "Airplane Propellers," *Aerodynamic Theory*, ed. W. F. Durand, New York 4, Div. L, 1963, pp. 128–143.

[9]Jimenez, A., Crespo, A., Migoya, F., and Garcia, J., "Large-eddy simulation of spectral coherence in a wind turbine wake," *Env. Research Letters*, Vol. 3, 2008.

[10]Sørensen, J. N. and Myken, A., "Unsteady actuator disc model for horizontal axis wind turbines," *J. of Wind Eng. and Ind. Aerodynamics*, Vol. 39, 1992, pp. 139–149.

[11]Mikkelsen, R., *Actuator Disc Methods Applied to Wind Turbines*, Ph.D. thesis, Technical University of Denmark, 2003.

[12]Sorensen, J. N. and Shen, W. Z., "Numerical modelling of Wind Turbine Wakes," *J. Fluids Eng.*, Vol. 124, 2002, pp. 393–399.

[13]Troldborg, N., *Actuator Line Modeling of Wind Turbine Wakes*, Ph.D. thesis, Technical University of Denmark, 2008.

[14]Fischer, P., Lottes, J., Pointer, D., and Siegel, A., "Petascale Algorithms for Reactor Hydrodynamics," *J. Phys. Conf. Series*, 2008.

[15]Fischer, P., Pointer, D., Obabko, A., Smith, J., and Childs, H., "Simulation of Turbulent Diffusion in 217-pin Wire-Wrapped Sodium Fast Reactor Fuel Assemblies," Tech. Rep. ANL-AFCI-267, 2009, DOE Advanced Fuel Cycle Initiative.

[16]Kerkemeier, S. G., *Direct Numerical Simulation of Combustion on Petascale Platforms: Applications to Turbulent Non-Premixed Hydrogen Autoignition*, Ph.D. thesis, ETH Zürich, 2010.

[17]Kerkemeier, S., Parker, S., and Fischer, P. F., "Scalability of the Nek5000 spectral element code," Jülich Blue Gene/P Extreme Scaling Workshop 78–11, 2010, Forschungszentrum Jülich.

[18]Patera, A. T., "A Spectral Element Method for Fluid Dynamics: Laminar Flow in a Channel Expansion," *J. Comp. Phys.*, Vol. 54, 1984, pp. 468–488.

[19]Fischer, P. F. and Patera, A. T., "Parallel Spectral Element Solution of the Stokes Problem," *J. Comp. Phys.*, Vol. 92, 1991, pp. 380–421.

[20]Fischer, P., "An Overlapping Schwarz Method for Spectral Element Solution of the Incompressible NavierStokes Equations," *J. Comp. Phys.*, Vol. 133, 1997, pp. 84–101.

[21]M. Deville, P. F. and Mund, E., *High-order methods for incompressible fluid flow*, Cambridge University Press, 2002.

[22]Fischer, P. and Mullen, J., "Filter-based stabilization of spectral element methods," *Comptes rendus de lAcadémie des sciences, Série I- Analyse numérique*, Vol. 332, 2001, pp. 265–270.

[23]Martinez, L. A., Leonardi, S., Churchfield, M. J., and Moriarty, P. J., "A Comparison of Actuator Disk and Actuator Line Wind Turbine Models and Best Practices for Their Use," AIAA Paper 2012-0900, 2012.

[24]Betz, A., *Introduction to the theory of flow machines*, Oxford: Pergamon Press, 1966.

[25]Çetin, N. S., Yurdusev, M. A., Ata, R., and Özdemir, A., "Assessment of Optimum Tip Speed Ratio of Wind Turbines," *Math. Comp. Appl.*, Vol. 10, 2005, pp. 147–154.

[26]Ragheb, M. and Ragheb, A. M., "Wind Turbines Theory - The Betz Equation and Optimal Rotor Tip Speed Ratio," *Fundamentals and Advanced Topics in Wind Power*, ed. Rupp Carriveau, InTech, ISBN 978-953-307-508-2, 2011, pp. 203–261.